Properties of isolated DNA bases, base pairs and nucleosides examined by laser spectroscopy

E. Nir[1], Ch. Plützer[2], K. Kleinermanns[2,a], and M. de Vries[3]

[1] Department of Chemistry, The Hebrew University, Jerusalem 91904, Israel
[2] Institut für Physikalische Chemie und Elektrochemie I, Heinrich Heine Universität Düsseldorf, 40225 Düsseldorf, Germany
[3] Dept. of Chemistry and Biochemistry, Santa Barbara, California 93106, USA

Abstract. The vibronic spectra of laser desorbed and jet cooled guanine (G) adenine (A), and cytosine (C) consist of bands from four, two and two major tautomers respectively, as revealed by UV–UV and IR–UV double resonance spectroscopy. The vibronic spectrum of adenine around 277 nm consists of weak $n\pi^*$ and strong $\pi\pi^*$ transitions, based on IR–UV and deuteration experiments. Precise ionization potentials of G and A were determined with 2-color, 2-photon ionization. We also measured vibronic and IR spectra of several base pairs. GC exhibits a HNH$\cdots$OH/NH$\cdots$N/C=O$\cdots$HNH bonding similar to the Watson-Crick GC base pair but with C as enol tautomer. One GG isomer exhibits non-symmetric hydrogen bonding with HNH$\cdots$N/NH$\cdots$N/C=O$\cdots$HNH interactions. A second observed GG isomer has a symmetrical hydrogen bond arrangement with C=O$\cdots$NH/NH$\cdots$O=C bonding. Two CC isomers were observed with symmetrical C=O$\cdots$NH/NH$\cdots$O=C bonding and nonsymmetrical C=O$\cdots$HNH/NH$\cdots$N interaction, respectively. Guanosine (Gs), 2-DeoxyGs und 3-DeoxyGs each exhibit only one isomer in the investigated wavelength range around 290 nm with a strong intramolecular sugar(5-OH)$\cdots$enolguanine(3-N) hydrogen bond.

PACS. 33.20.Lg Ultraviolet spectra

1 Introduction

The DNA bases have been the subject of many theoretical and experimental investigations because of their biological importance [1–4]. In the gas phase the intrinsic properties of the bases can be studied without intermolecular interactions at vibrational or even rotational resolution [5–14]. Though small they are difficult to vaporize without extensive decomposition. Especially guanine cannot be vaporized intactly by simple thermal heating. Recently, the vibronic spectrum of laser desorbed, jet cooled guanine was obtained based on resonance enhanced 2-photon ionization detection at the parent mass [15]. These pioneering studies were followed by a number of investigations of guanine [16–18], guanine base pairs [19–21], guanosine [22], adenine [23–25] and cytosine [26] based on resonant two-photon ionization. The results showed that nucleobases and complexes composed of paired bases can be studied in the absence of external effects like solvent interactions and collective modes of the DNA backbone. Important conclusions with regard to the photochemical stability and different tautomers of the bases and hydrogen bond arrangements of the base pairs can be drawn. In this paper we critically discuss and compare these results and present

new measurements and calculations shining more light on the intrinsic properties of these important biomolecular building blocks.

2 Experimental and theoretical methods

The measurements with laser desorbed nucleobases were performed with an apparatus described in detail elsewhere [27]. In short, material is laser desorbed from a graphite sample in front of a pulsed nozzle, as indicated in Figure 1. Typical fluences of the Nd:YAG desorption laser operated at 1 064 nm (where graphite absorbs but the nucleobases do not) are about 1 mJ/cm^2 or less, which is considerably lower than the fluences normally used for ablation. The laser is focused to a spot of about 0.5 mm diameter within 1 mm in front of the nozzle. We used a pulsed valve (General Valve; Iota One) with a nozzle diameter of 1 mm at a backing pressure of about 5 atm argon drive gas. In some experiments we used CO$_2$ as a drive gas to obtain more intense spectra. The ionization laser crosses the skimmed molecular beam at right angles inside the source region of a reflectron time-of-flight (TOF) mass spectrometer. We obtained mass selected excitation spectra by monitoring specific selected mass peaks, such as $m/e = 151$ for guanine, while varying the two-photon,

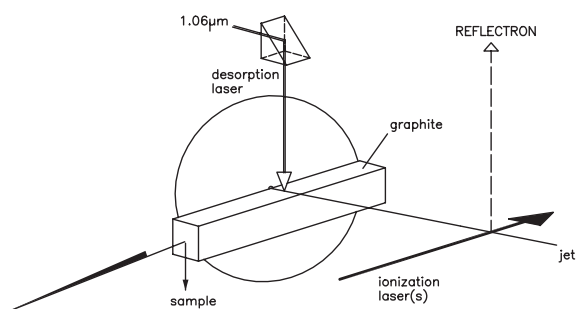[a] e-mail: `kleinermanns@uni-duesseldorf.de`

Fig. 1. Scheme of the experimental arrangement used for laser desoption.

Fig. 2. Scheme of resonant two-photon ionization (R2PI) and UV–UV and IR–UV double resonance spectroscopy.

one-color ionization wavelength (Resonant Two-Photon Ionization: R2PI). Adenine was thermally evaporated at 210–240 °C in the pulsed jet of a linear TOF mass spectrometer as described in detail elsewhere [28].

The double resonance experiments were performed with the same set up in both machines, as indicated in Figure 2. We performed Spectral Hole Burning (SHB; double resonance is used as synonym) by using two counterpropagating dye laser pulses with a relative delay of about 150 ns. This results in two peaks in the TOF spectrum – the first from the "burn" laser and the second from the "probe" laser. When both lasers are tuned to a resonance of the same isomer, the burn laser causes a decrease in the signal of the probe laser, because it depletes the common ground state. We scan the burn laser while the probe laser frequency is fixed to an intense band of one isomer. If a significant band of the R2PI spectrum is missing in the burn spectrum it belongs to another isomer. In the next step we probe at this frequency while scanning the pump laser to reveal the spectrum of the next tautomer.

We performed IR–UV SHB with the same method employing a difference frequency IR laser as the burn laser. The radiation from an infrared dye (a mixture of Styryl 8 and Styryl 9) was aligned collinearly with the perpendicularly polarized Nd–YAG fundamental (1 064 nm) and directed through a MgO-doped $LiNbO_3$ crystal to generate tunable IR light from 3 300 to 4 000 cm^{-1}. Suitable dielectric mirrors separate the Nd–YAG fundamental and the dye laser beam from the IR beam. We typically use 50 mJ of the YAG fundamental and 10 mJ of the dye laser to obtain around 1 mJ/pulse IR radiation from 3 300 to 4 000 cm^{-1} with a bandwidth of < 0.1 cm^{-1}. The IR laser was calibrated by recording a water vapor spectrum. Color centers in the $LiNbO_3$ crystal lead to a decrease of the IR intensity between 3 515 and 3 550 cm^{-1}. In that spectral range we used another $LiNbO_3$ crystal with a gap in another region.

The calculations were been carried out using the Gaussian 98 program package [29]. We performed Møller-Plesset second order perturbation theory (MP2) calculations utilizing a 6-311G(d,p) basis set for guanine and adenine monomers and calculations on the HF 6-31 G(d,p) level for guanosine and the clusters. All structures have been fully optimized on the respective level with 10^{-8} hartree as SCF convergence criterion and
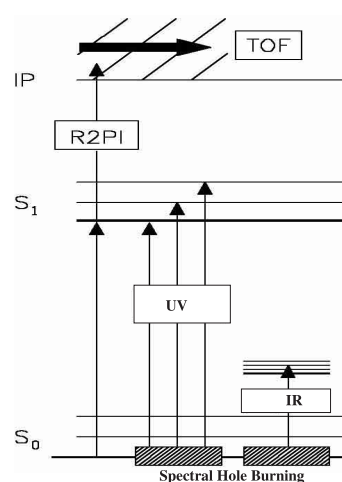
1.5×10^{-5} hartree/bohr and hartree/degree, respectively, as convergence criteria for the gradient optimization of the structures. The vibrational frequencies were obtained by performing a normal mode analysis on the optimized geometries using analytical gradients of the energy. The stabilization energies were corrected for the zero point energy (ZPE) using the harmonic frequencies calculated at the respective level of theory. The dissociation energies D_0 of the clusters were further corrected for the Basis Set Superposition Error (BSSE).

3 Results and discussion

3.1 Guanine

Tautomers of the nucleobases play an important role in substitution mutations. Guanine has the possibility of oxo $\leftrightarrow$ hydroxy, amino $\leftrightarrow$ imino, N1H $\leftrightarrow$ N3H and N7H $\leftrightarrow$ N9H prototropy and is therefore the nucleobase with the largest number of possible tautomeric forms. Recently the vibronic spectrum of guanine was obtained based on gentle laser desorption of this fragile molecule in a jet and R2PI detection at the parent mass [15]. In a subsequent publication Piuzzi *et al.* [30] claimed that the spectrum arises from three different tautomers which were identified by UV–UV SHB and fluorescence decay times of 12, 22 and 360 ns for their origin transitions at 32 864 (A), 33 269 (B) and 33 491 cm^{-1} (C). They tentatively assigned tautomer A and B to N7H/N9H keto guanine and tautomer C to one of the enol forms based on the spectral shifts and lifetimes [30]. Nir *et al.* [16] disproved this assignment. They identified three different tautomers by UV–UV and IR–UV SHB with origin transitions at 32 870 (1), 33 275 (2) and 33 914 cm^{-1} (3), *cf.* Figure 3. Tautomer 1 shows IR bands at 3 587, 3 577, 3 516 and 3 462 cm^{-1}, *cf.* Figure 4. Tautomers 2 and 3 have their two highest frequencies at 3 505/3 490 cm^{-1} and 3 505/3 497 cm^{-1}, respectively, which is very similar to those for the two tautomers of 1-methylguanine (enol
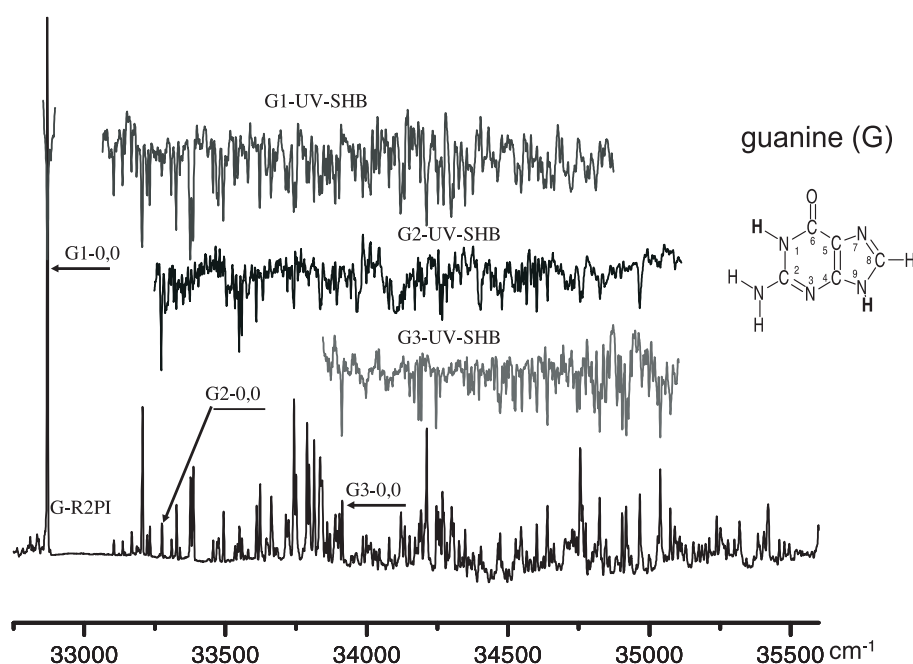
Fig. 3. R2PI and UV–UV double resonance spectra of guanine revealing three major tautomers in the investigated wavelength range. The R2PI spectrum is displayed in the lower trace. The upper traces show the decrease of the ion intensity induced by the probe laser when the pump laser is scanned (SHB spectra).

form blocked) with highest frequencies of $3\,505/3\,489$ and $3\,505/3\,495$ cm^{-1} [16]. Since methylation in position 1 corresponds to blocking the enol form, this similarity strongly suggests that tautomers 2 and 3 are the keto tautomers. The calculated frequencies in Figure 4 indeed show that the NH-stretch vibrations have lower frequencies in the keto tautomers than in the enol tautomers. The highest frequency in the spectrum of tautomer 1 is at $3\,587$ cm^{-1} and can be assigned to the OH stretch vibration of the enol form which is absent in the keto form. Hence the assignment to keto and enol forms is consistent and the assignment of tautomer 1 (tautomer A in Ref. [30]) to a keto tautomer was disproved. The band at $33\,491$ cm^{-1} (tautomer C with 360 ns lifetime in Ref. [30]) was later ascribed to the fluorescence of small carbon clusters formed from the graphite powder used as desorption matrix [31].

Our assignment of tautomer 1, 2, 3 to enol, keto, keto forms was acknowledged very recently by Mons *et al.* [31]. They reported a fourth tautomer with origin transition at $34\,755$ cm^{-1} [31] and ascribed it to another enol tautomer based on the similarity of its IR spectrum with our IR spectrum of tautomer 1, *cf.* Figure 4. In reference [16] we proposed an assignment of the observed tautomers to 7H/9H forms which was clearly less certain than our keto/enol assignment and mainly based on calculated stabilities and frequencies. Mons *et al.* revised our proposal [31] and assigned tautomer 1 to N7H enol, tautomer 2 to N7H keto, tautomer 3 to N9H keto and tautomer 4 to N9H enol (*cis* or *trans*). Their assignment is based on the very similar IR and UV absorption frequencies of the 9-methyl-and 7-methylguanine tautomers compared to the corresponding guanine tautomers. The 7H/9H assignment of the enol tautomers is consistent in-

validating our proposal that the enol tautomer in Figure 4 has the H atom in position 9 [16]. The 7H/9H keto assignment however is based on a comparison with a single IR band of merely 7-methylguanine keto (9-methylguanine keto could not be detected) with the keto guanines at very low signal-to-noise level and large nearby spectral gap of IR laser power. We have hints from our (methylated) guanine dimer [20] spectra that the 7H/9H keto assignment is reversed compared to reference [31] and will therefore repeat the 7-methylguanine keto IR–UV measurements at better spectral quality and without spectral gap.

Two remarkable facts remain. Firstly one of the two N9H enol rotamers (*cis* or *trans*) is still missing. These rotamers have nearly identical calculated stabilization energies [16] and have been identified with comparable abundances in IR matrix studies of 9-methylguanine [32,33]. No vibronic bands of this further N9H enol rotamer has been detected up to now. Secondly the electronic spectrum of the biologically relevant keto form of 9-methylguanine could not be detected yet [31]. We can speculate about a particular short lived excited state of this molecule and that nature has selected 9-substituted keto guanines for protection against photochemistry. We return to this topic when we discuss guanosine where a sugar molecule substitutes in position 9 and where again only the guanine enol form of guanosine could be detected.

3.2 Guanine-cytosine

We can form individual GC base pairs by desorbing from a mixture of guanine and cytosine on graphite and allowing the formation of clusters in the jet expansion. By recording
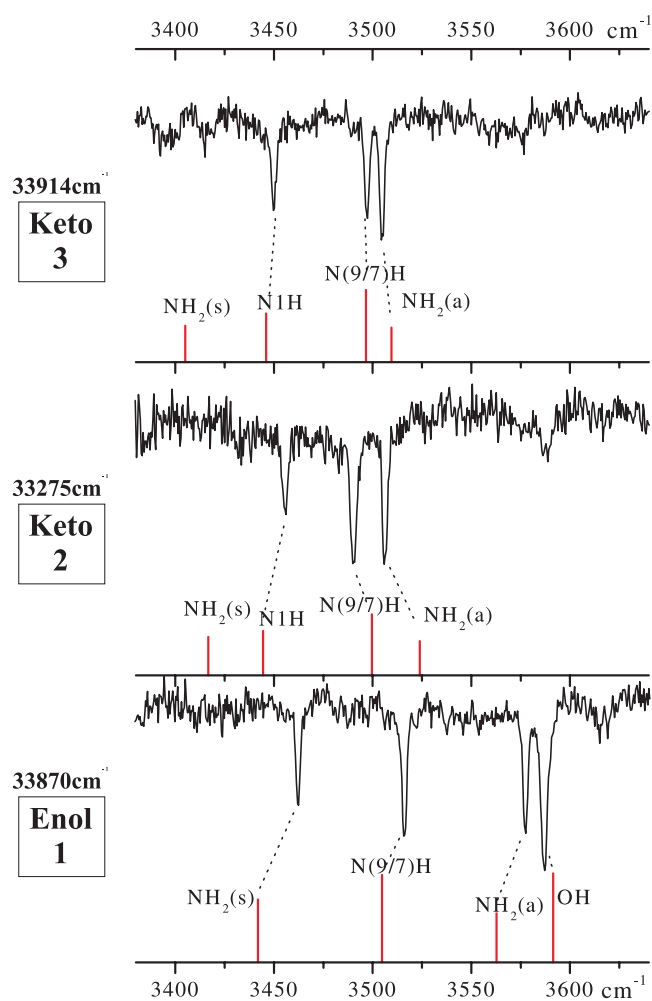
Fig. 4. IR–UV double resonance spectra of the guanine tautomer analysed at $32\,870$ cm^{-1} (enol 1), $32\,870 + 405$ cm^{-1} (keto 2) and $32\,870 + 1\,044$ cm^{-1} (keto 3). The vibrational frequencies calculated at the MP2 level are shown for comparison. The calculated frequencies are scaled with a factor 0.942 for OH stretching and 0.951 for NH stretching vibrations obtained from a comparison of the experimental para-aminophenol IR spectrum [52] with the spectrum calculated at the MP2/6-31G(d,p) level.

R2PI spectra at the GC cluster mass (262 amu) we obtained a vibronic spectrum of GC [21]. The SHB measurements showed that only one isomer of GC absorbs in the investigated wavelength range from $33\,200$ to $34\,100$ cm^{-1}. Figure 5 shows the IR-UV spectrum of GC [21]. We calculated more than 60 possible isomeric structures of GC and performed normal mode vibrational analysis at the isomer minima. The experimental IR spectrum does not agree with the calculated IR spectrum of the most stable Watson-Crick cluster arrangement. Instead the observed GC isomer exhibits a HNH$\cdots$OH/NH$\cdots$N/C=O$\cdots$HNH bonding similar to the Watson-Crick G–C bonding but with C in enol tautomeric form [21], compare also for the OH stretch frequency in the IR spectrum of C-C5M "red" in Figure 11. Recently we observed another GC isomer

which absorbs at around $32\,800$ cm^{-1}. Our preliminary data suggest that it is again not the Watson-Crick pair.

The 6 intermolecular vibrations of GC reflect the loss of three rotations and three translations upon complex formation and are displayed schematically in Figure 6. Figure 7 shows the experimental intermolecular vibrations of the observed G–C base pair in the S_1 state. The two low frequency peaks in the spectrum below 20 cm^{-1} are absent when we use krypton as the drive gas instead of argon. This suggests that they may be due to hot bands or result from dissociating clusters with argon, rather than to G–C vibrations. The bands at 68, 82, 115 and 120 cm^{-1} may be assigned to step, gearing, antisymmetric and symmetric stretch vibrations in the S_1 state, respectively. The agreement between the experimental (S_1 state) and calculated (S_0 state) vibrational pattern is not very good and other G–C pairs match the experimental pattern just as well or better. Unfortunately, quality *ab initio* calculations of the S_1 state vibrations of a cluster the size of G–C are out of reach at the moment. For this reason the intermolecular vibrations in the S_1 state cannot yet be called on for structural assignment.

3.3 Guanine-guanine

At optimized desorption conditions with the graphite substrate positioned close to the jet and at somewhat increased desorption laser power we observed GG ion signals at $m/e = 302$. SHB of the vibronic spectrum (not shown here) exhibits that two GG isomers absorb in the investigated spectral region $32\,565$ to $33\,600$ cm^{-1}. Figure 8 shows the two IR spectra obtained by IR–UV SHB [20]. The comparison of experimental and calculated vibrational frequencies shows that the most stable form K9K9-1 is not observed. GG1 exhibits a nonsymmetric hydrogen bonding with HNH$\cdots$N, NH$\cdots$N and O=C$\cdots$HNH interactions (K9K7-2 or K7K7-2). The other isomer has a symmetrical hydrogen bond arrangement with C=O$\cdots$NH/NH$\cdots$O=C bonding (K9K7-1). The most stable guanine dimer forms C=O$\cdots$NH/NH$\cdots$O=C hydrogen bonds and has C_{2h} symmetry (K9K9-1). Possibly its UV spectral shift is strong mainly due to different hydrogen bond strengths in the electronic ground and excited state and the allowed S_0-S_2 transition (exciton splitting) outside of the investigated spectral range. The shift may be similar to that in the 2-pyridon dimer $(2PY)_2$ which also has a symmetrical C=O$\cdots$NH/NH$\cdots$O=C hydrogen bond and C_{2h} symmetry. Its S_0-S_2 origin band is at $30\,776$ cm^{-1} while the 2PY monomer absorbs at $29\,831$ cm^{-1} [34] (a second conformer absorbs at $29\,930$ cm^{-1}). An other possible reason for not observing the K9K9-1 spectrum, in spite of the expectation that this structure should be formed preferentially in the jet, is reduced stability in the S_2 or ionic state.

3.4 Guanosine

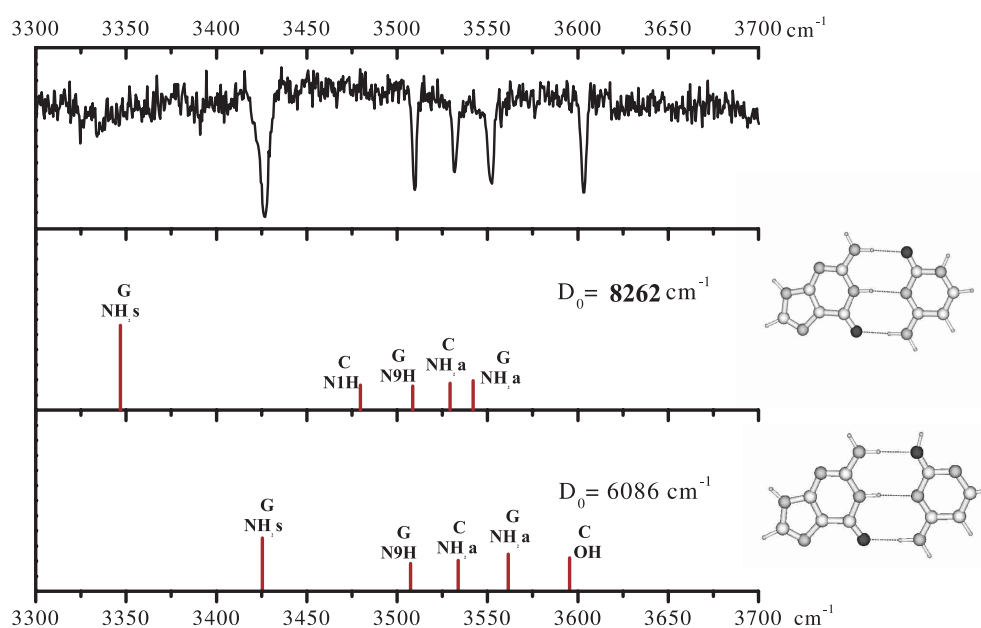The REMPI spectroscopy of laser desorbed guanosine (Gs), 2-deoxyguanosine (2-DeoxyGs) and

Fig. 5. IR–UV double resonance spectra of the observed G–C isomer. The IR spectra of 60 different GC structures have been calculated and compared to the experimental IR spectrum. The vibrational frequencies of the most stable Watson-Crick dimer (middle trace) and the dimer with best agreement to the experimental IR spectrum (lower trace) are displayed. The frequencies are calculated at the HF/6-31G(d,p) level and scaled with a factor 0.893 for all NH stretching frequencies and 0.867(0.866) for the OH stretching frequency of enol guanine (enol cytosine) obtained from the best fit to the experimental guanine and cytosine monomer frequencies. All values are in cm^{-1}.
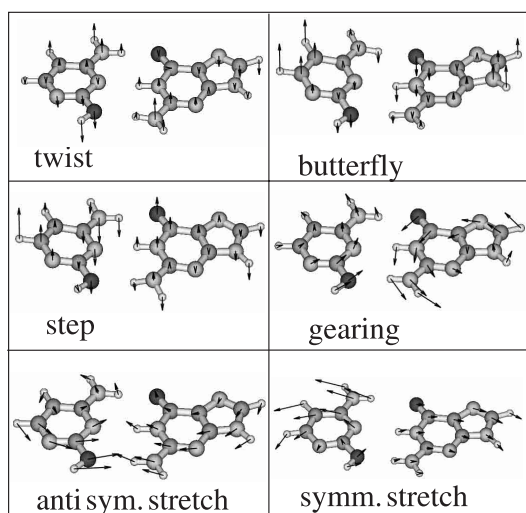

Fig. 6. Intermolecular vibrations. These are the out-of-plane torsion or twisting mode, the out-of-plane bending (butterfly) motion with the guanine and cytosine moieties as wings, the antisymmetric out-of-plane bending (alternating stairs or step) motion, the in-plane bending (gearing) motion of the two moieties and the antisymmetric and symmetric stretching vibrations.

3-deoxyguanosine (3-DeoxyGs) has already been published [22]. In that paper we proposed 2 conformers contributing to the vibronic spectra of Gs and 3-DeoxyGs but recently we found by UV–UV hole burning that each of the 3 spectra correlate with the same ground state.

This suggests a single conformation or isomerization on the 150 ns timescale of the delay between burn and probe lasers. Figure 9 shows the corresponding IR–UV spectra. For comparison the IR spectra of 2,3-isopropylGs and G(enol, keto) are shown as well. In 2,3-isopropylGs the OH group of the sugar moiety in position 2 and 3 is blocked. Therefore its IR spectrum does not exhibit the corresponding OH vibrations but agrees well with the G(enol) spectrum (aside from the N9–H stretching vibration which is absent because of sugar substitution in that position). Clearly the enol and not the keto tautomer of guanine is the chromophore in all 4 Gs species. The OH group in position 5 of 2,3-isopropylGs is not blocked by substitution and should therefore show an IR band. Our calculations [22] however show that the most stable Gs conformer forms a strong intramolecular hydrogen bond between the sugar 5-OH and 3-N guanine, as indicated in the inset in Figure 9. A hydroxyl group which is tightly H bonded to nitrogen shows a strong red shift of its stretching vibration and absorbs probably outside of the investigated IR spectral range [35,36].

The IR spectra of the other guanosines support the supposed Gs structure (inset of Fig. 9) which is the most stable one according to our *ab initio* calculations [22]. In 3-DeoxyGs we observe an additional OH vibration compared to 2,3-isopropylGs at a higher frequency which is obviously from free (not hydrogen bonded) OH in position 2 of the sugar moiety. In 2-DeoxyGs there is an additional OH vibration near to the 2-OH vibration which can be traced to the 3-OH stretching vibration. The IR spectrum of Gs in the range of the OH and NH stretching vibrations
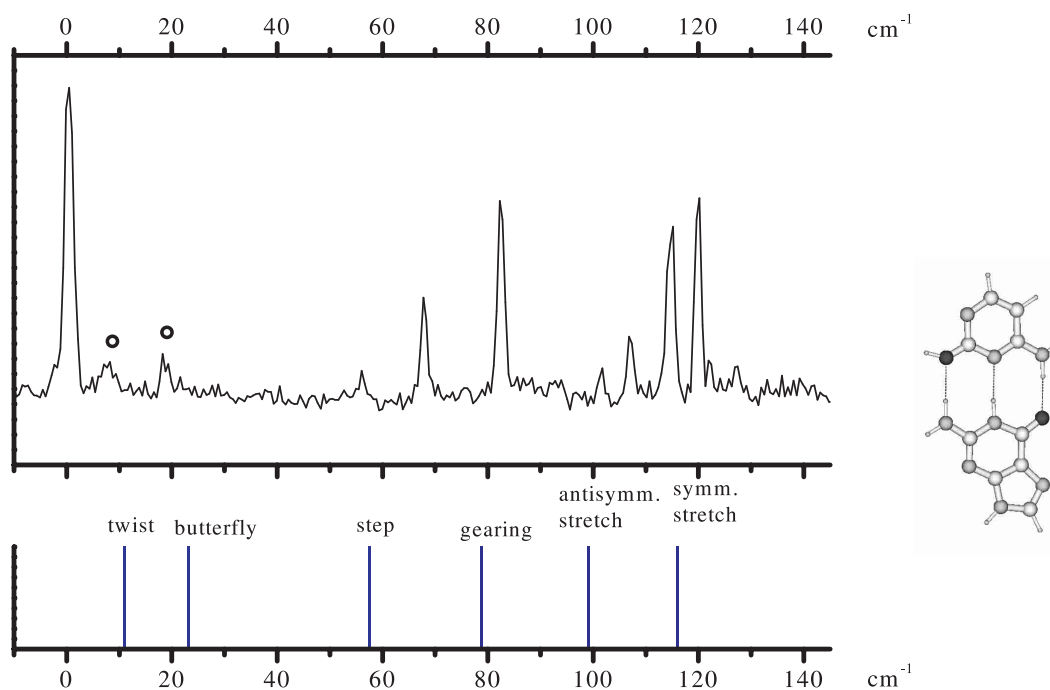
Fig. 7. Vibronic spectrum of the observed G–C isomer in the frequency range of the intermolecular vibrations. The unscaled frequencies of the intermolecular vibrations calculated at the HF/6-31G(d,p) level are shown for comparison. The spectrum is displayed relative to the electronic origin at $33\,314$ cm^{-1}. The bands marked with circles are absent when we use krypton as the drive gas instead of argon and may be due to hot bands or result from dissociating clusters with argon.
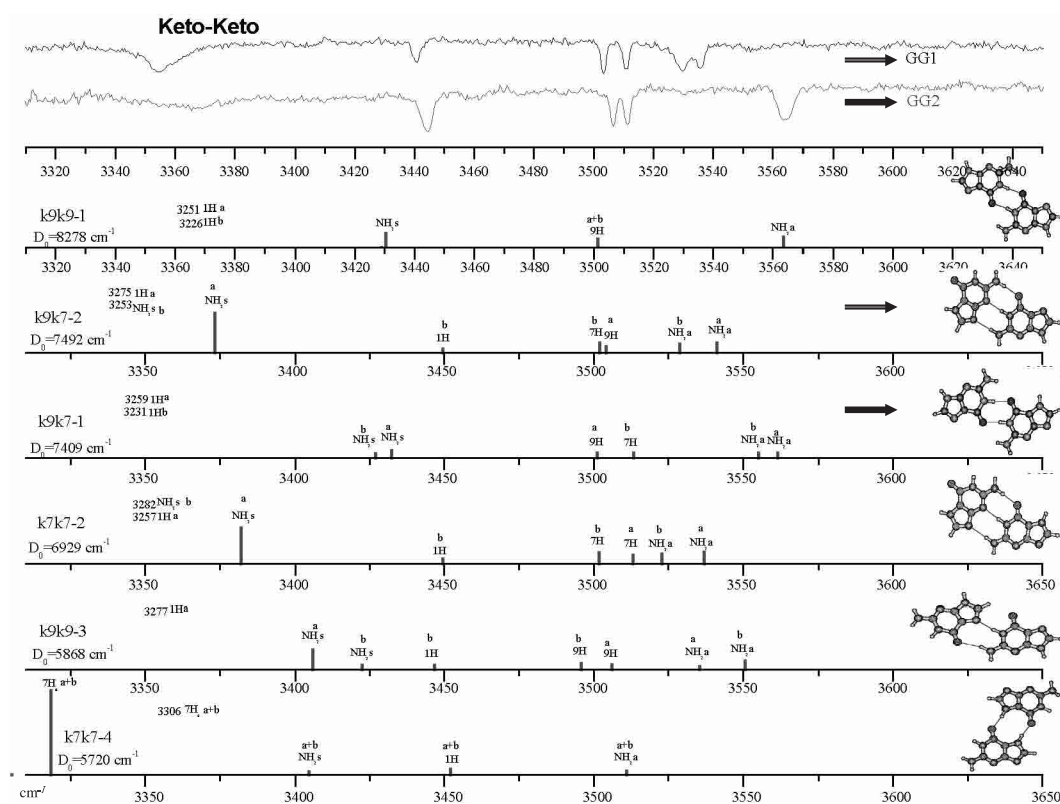

Fig. 8. The infrared spectra (IR–UV SHB) of the two isomers of the guanine dimer analysed at $33\,103$ cm^{-1} (GG1) and $33\,282$ cm^{-1} (GG2). The vibrational frequencies of the most stable keto-keto dimers calculated at the HF/6-31G(d,p) level are shown for comparison. The calculated frequencies are scaled with a factor 0.893 obtained from the best fit of the guanine monomer frequencies to the frequencies calculated at the HF/6-31G(d,p) level.
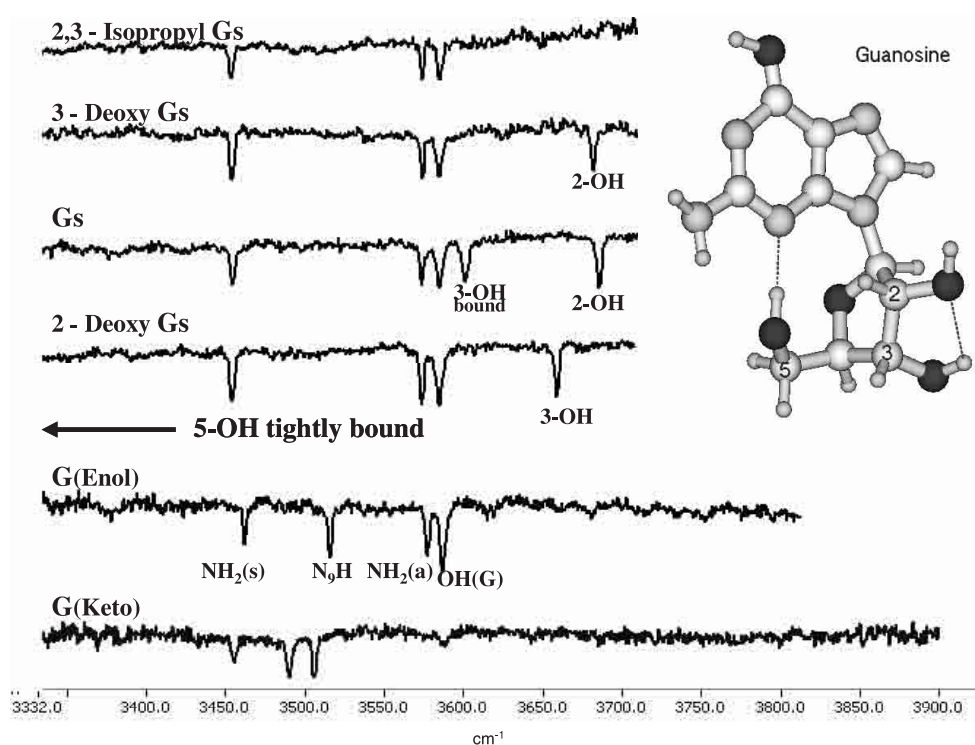
Fig. 9. The IR–UV spectra of laserdesorbed guanosine (Gs), 2-deoxyguanosine (2-deoxyGs) and 3-deoxyguanosine (3-deoxyGs). For comparison the IR spectra of 2,3-isopropylGs and G(enol, keto) are shown also. The inset shows the most stable guanosine structure at the HF/6-31G(d,p) level in agreement with the observed IR bands. For discussion see text.
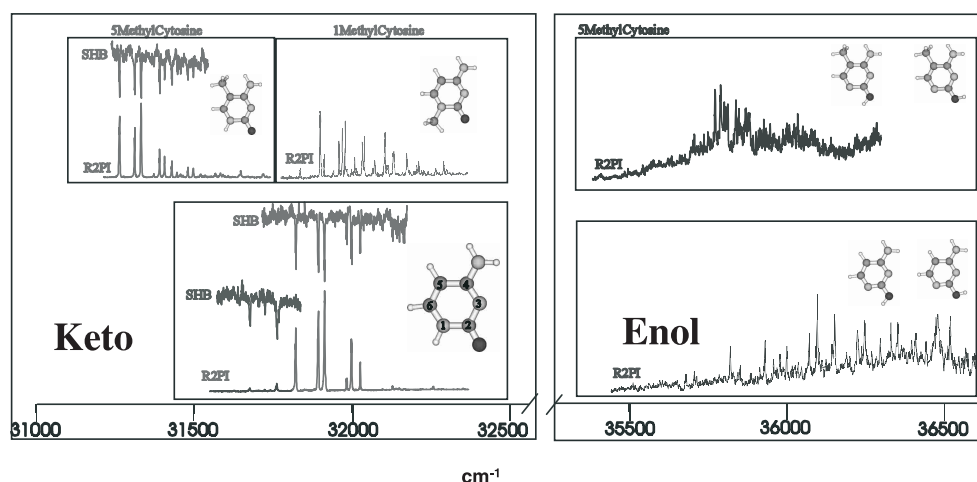

Fig. 10. R2PI and UV–UV SHB spectra of cytosine, 1-methylcytosine and 5-methylcytosine.

consists of the G(enol) spectrum without N9H vibration, the 2-OH vibration of the sugar moiety and a vibration somewhat red shifted to free 3-OH, which is probably from 3-OH involved in a weak intramolecular hydrogen bond to 2-OH [37] as displayed in Figure 9. Preliminary calculations of the vibrational frequencies support this view.

The electronic origins of guanosine are at $34\,443$ cm^{-1} [22], 9-methylguanine enol at $34\,612$ cm^{-1} [31], 9-guanine enol at $34\,755$ cm^{-1} [31], 7-methylguanine enol at $32\,561$ cm^{-1} [31] and 7-guanine enol at $32\,870$ cm^{-1} [16] so that substitution in position 9 obviously shifts the electronic spectra of enol guanine very much to the blue.

We were not able to detect keto guanosine yet. Similarly it was reported in reference [31] that the keto form of 9-methylguanine could not be observed. Possible reasons are ionization potentials of the 9-substituted keto guanines which are too high for efficient 2-photon-1 color ionization or particularly short lived excited states.

3.5 Cytosine

Cytosine (C), unlike other pyrimidine bases, exhibits vibronic spectra with sharp features in two spectral regions, separated by about $4\,000$ cm^{-1}, *cf.* Figure 10 and reference [26]. 5-methylC exhibits spectra in both
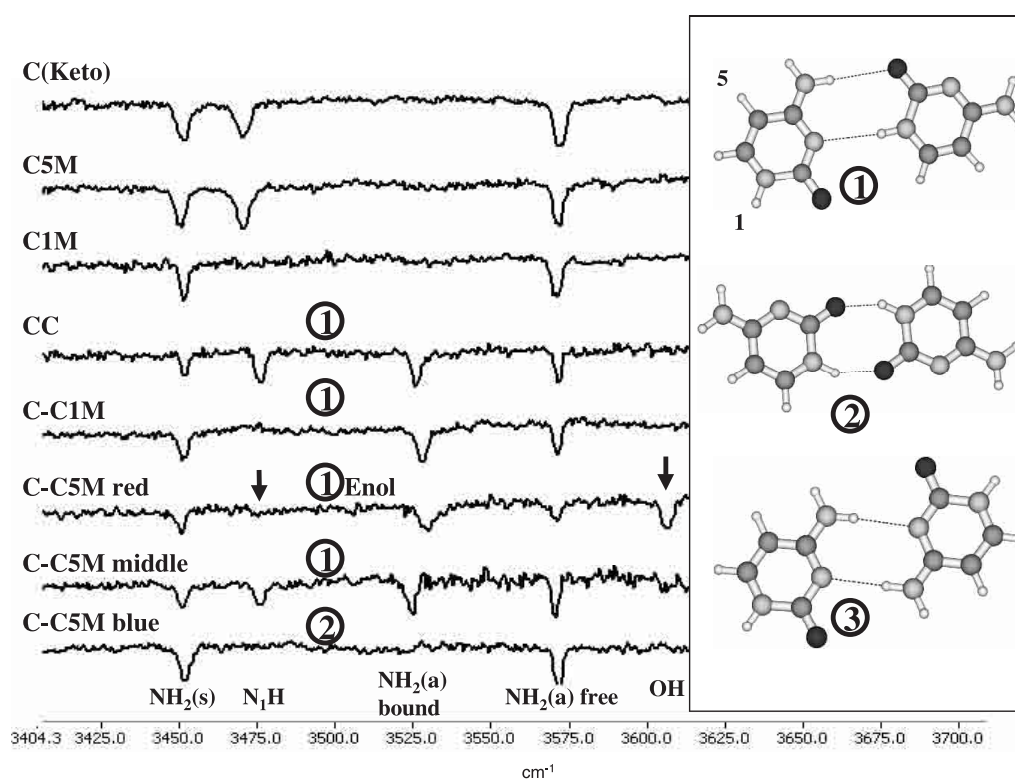
Fig. 11. IR–UV spectra of cytosine (keto tautomer; see text), 5-methylcytosine and 1-methylcytosine and dimers of cytosine, cytosine-1-methylcytosine and cytosine-5-methylcytosine. The inset displays the 3 most stable dimer structures according to molecular dynamics/quenching calculations [39]. 1, 2, 3 indicates the assignment of the IR spectra to specific cluster structures, see text.

these spectral regions while 1-methylC in which the enol form is blocked absorbs only in the region around $32\,000$ cm^{-1}. Therefore we assign the vibronic spectrum around $32\,000$ cm^{-1} to the keto tautomer of C and the spectrum around $36\,000$ cm^{-1} to the enol tautomer of C. This interpretation is supported by the IR–UV spectrum of the C tautomer absorbing around $32\,000$ cm^{-1} which is displayed in Figure 11. The spectrum shows the anti-symmetric and symmetric NH$_2$ and the N1H stretching vibrations at their typical frequencies but not the OH vibration. The 5-methylC and 1-methylC tautomers absorbing around $32\,000$ cm^{-1} exhibit a very similar IR spectrum as C(keto), merely the N1H vibration is missing in 1-methylC. Our results agree with the microwave spectroscopical investigations in reference [14] where the keto and enol (OH *cis* to N1) cytosine tautomers were measured to have similar abundances whereas the population of the keto-imine tautomer is only one quarter of that of the other tautomers, compare also for the keto-enol forms of 2-pyridone [38]. We have no IR-UV spectra of the "blue" spectrum of cytosin yet. The CC dimer spectra however show that we indeed have the enol tautomer in the jet, *cf.* Figure 11.

3.6 Cytosine-cytosine

The cytosine dimer CC absorbs around $33\,500$ cm^{-1} and its UV–UV SHB spectrum exhibits only one isomer in this spectral region. The corresponding IR spectrum is shown in Figure 11. The inset displays the 3 most stable dimer structures according to molecular dynamics/quenching calculations with an empirical force field and correlated *ab initio* quantum chemical calculations from the Hobza group [39]. The CC IR spectrum shows the same frequencies as the C(keto) spectrum with an additional band at $3\,525$ cm^{-1} which lies in the typical frequency range of an antisymmetric NH$_2$ stretching vibration of a NH$_2$ group involved in a hydrogen bond with a C=O group, such as the GG1 and k9k7-2 spectra in Figure 8. Hence the CC IR spectrum suggests a combination of 1 free and 1 bound NH$_2(a)$ vibration which occurs only in the most stable cluster 1 in Figure 11. The 1-methylcytosine – cytosine dimer (C-C1M) shows the same spectrum as CC, however without the free N1H vibration. In cluster 1 there is only one free N1H group, which is blocked by methylation in the case of C-C1M.

The vibronic spectrum of 5-methylcytosine – cytosine (C-C5M) has contributions from 3 isomers as determined by UV-UV SHB measurements (not shown here). C-C5M "red" absorbs at around $32\,500$ cm^{-1} and shows the same spectrum as CC except that the N1H vibration is missing and there is an additional free OH vibration, marked by arrows in Figure 11. This agrees with structure 1, however with one C in the enol form (the one with N1H not involved in a hydrogen bond). C-C5M "middle" absorbs at around $32\,700$ cm^{-1} and shows exactly the same IR
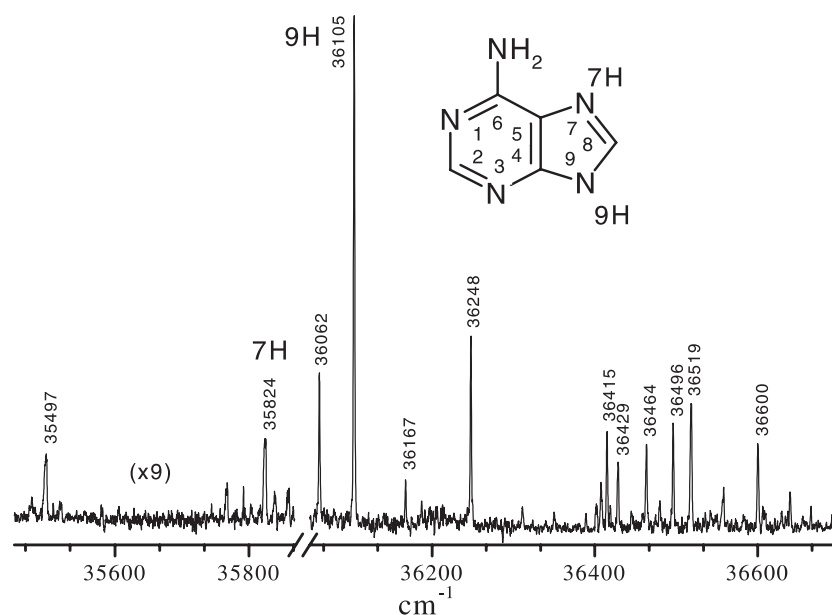
Fig. 12. R2PI spectrum of adenine. For explanation see text.

spectrum as CC. Hence this isomer can be assigned to structure 1 with one of the C methylated in position 5. C-C5M "blue" absorbs at around $32\,900$ cm^{-1} and shows no free OH, free N1H and bound NH$_2$ vibrations in the investigated IR range in agreement with the symmetrical structure 2. Here only the coupled free NH$_2$ vibrations with reversed phase are infrared allowed and only one NH$_2(a)$ and NH$_2(s)$ band is observed. The N1H vibrations are involved in strong symmetrical hydrogen bonds and are probably shifted below $3\,400$ cm^{-1}. Hence we conclude that we observe the two most stable dimers in excellent agreement with the calculations in reference [39]. We cannot exclude that dimer 3 which has similar stability than dimer 1 and 2 [39] absorbs in another part of the UV spectrum which is not yet investigated.

3.7 Adenine

Figure 12 shows the one-color, two-photon ionization spectrum of adenine in the spectral range from $35\,450$ cm^{-1} to $36\,700$ cm^{-1} [25]. Our results show that the weak UV bands below $36\,050$ cm^{-1} observed by Kim *et al.* [23] are indeed reproducible. We were able to obtain these weak bands with sufficient intensity to perform IR–UV double resonance experiments by heating adenine up to 260 °C. In an earlier work [25] we showed that all more intense bands $> 36\,050$ cm^{-1} have the same IR spectra in the region of the NH vibrations (within the experimental uncertainty of ± 0.5 cm^{-1}) and thus belong to the same tautomer. The comparison with *ab initio* calculated stabilities and vibrational frequencies pointed to the most stable 9H-tautomer [25], shown in the upper spectrum of Figure 13. The weak UV band at $35\,497$ cm^{-1} in Figure 12 exhibit exactly this IR spectrum and thus belongs to the 9H-tautomer. The band at $35\,824$ cm^{-1} however has a very different IR pattern, shown in the
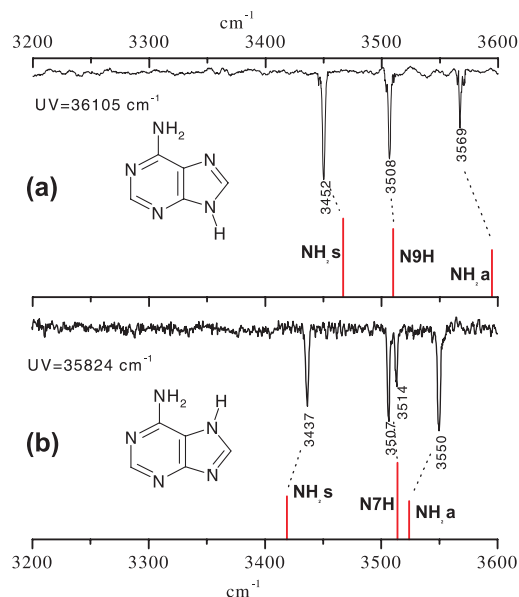

Fig. 13. IR–UV spectra of adenine analysed at $36\,105$ cm^{-1} (a) and $35\,824$ cm^{-1} (b). The IR bands can be assigned to the symmetric NH$_2$ stretch vibration at $3\,437$ and $3\,452$ cm^{-1}, the N7H/N9H stretch vibrations at $3\,507/3\,514$ and $3\,508$ cm^{-1} and the antisymmetric stretch vibrations at $3\,550$ and $3\,569$ cm^{-1} of the N7H and N9H tautomers, respectively. Possible reasons for the $3\,507/3\,514$ cm^{-1} splitting are discussed in the text. The vibrational frequencies calculated at the B3LYP/6-311G(d,p) level are shown for comparison. A scaling factor 0.9613 as recommended in reference [53] for B3LYP/6-31G(d) has been used. According to MP2 and B3LYP calculations with the split valence 6-311G(d,p) basis set 7H-adenine is 33 respectively 36 kJ/mol less stable (ZPE corrected) than 9H-adenine [25].

lower spectrum of Figure 13. Both the symmetric and antisymmetric NH_2 stretching vibrations are shifted to smaller frequencies ($3452/3437$ and $3569/3550$ cm^{-1}) while the N–H stretching vibration stays nearly the same (3508, $3514/3507$ cm^{-1}) in qualitative agreement with the B3LYP calculations for the 9H-/7H-tautomer, depicted as stick spectra in Figure 13. Probably the band at 35824 cm^{-1} in Figure 12 is a vibronic band of 7H-adenine and not its electronic origin which may be red shifted relative to 9H-adenine similar as 7H/9H enol guanine and is possibly not detected here due to an insufficient ionization energy.

Are the bands at $3514/3507$ cm^{-1} both from the N–H stretching motion? Deuteration experiments can answer this question. The d_0-band at 35824 cm^{-1} correlates with 4 bands in the d_1-isotopomers arising from substitution at the NDH, NHD, N7D and CD position (spectra not shown here). The IR/R2PI spectra taken from these 4 electronic origins helped to unambiguously identify the substitution position, because the respective ND vibration shifts below 3000 cm^{-1} outside of the investigated spectral range. The IR/R2PI spectrum of d_1-adenine taken *via* the electronic origin of the N7D isotopomer at 35829 cm^{-1} showed that the two bands at 3514 and 3507 cm^{-1} are both missing and can therefore be traced back to the N–D stretching vibration which is shifted below 3000 cm^{-1}. The symmetric and antisymmetric NH_2 stretching frequencies are unchanged at 3437 and 3550 cm^{-1}.

What is the reason for the $3507/3514$ cm^{-1} splitting of the N–H vibration in Figure 13b? The MP2 calculations show that the N9–H bond is in the plane of the ring system while the two H atoms of its NH_2 group are (nearly symmetric) slightly out of plane in the S_0 state. By contrast the H atom of the NH group of the 7H-tautomer lies out of plane with a dihedral angle of 11° and the neighboring H atom of the NH_2 group is more out of plane than the distant H atom by 45° and 7°, respectively. This is probably due to stearic hindrance between one H atom of the NH_2 group and the neighboring H atom in position 7. A concerted out of plane N–H bending and C–NH_2 torsion or NH_2 inversion would lead to a double minimum potential and possibly tunneling splitting. The bands at $3507/3514$ cm^{-1} could also arise from a Fermi resonance between a vibrational overtone or combination state and the N–H fundamental. This seems less probable because the corresponding splitting is absent in the N9H IR spectrum but cannot be excluded.

A question remains concerning the other weak bands below 36050 cm^{-1} in Figure 12. As already pointed out, the bands at 35497 and 36105 cm^{-1} have exactly the same IR spectra and therefore belong to the same tautomer (the N9H form) with a common electronic ground state. Experiments at different stagnation pressures in the range of 100 mbar to 2 bar showed that the intensity ratios of the bands at 35497, 36062, 36167, and 36248 cm^{-1} relative to the intense transition at 36105 cm^{-1} are independent of expansion cooling conditions. The band widths and the broadening with decreasing stagnation pressure are very similar as well. Therefore we conclude that these transi-

tions are not hot bands. The logical consequence is that they are transitions to an electronic state different from the 36105 cm^{-1} transition as proposed by Kim *et al.* [23].

What experiment could further test this hypothesis? We tried to obtain IR/R2PI spectra of the electronically excited state of these vibronic transitions by performing double resonance spectroscopy with zero time delay between the pump and probe lasers. No ion dips were obtained under these conditions probably due to the ps lifetime in the electronically excited state of adenine [24]. Deuteration experiments can provide another clue about the nature of the excited state. The spectral shifts of the different isotopomers depend on the difference between the vibrational zero point energies in the electronically excited and ground state. Figure 14 shows the electronic spectra of d_0-(undeuterated)adenine and d_1-adenine for comparison. The intense transition at 36105 cm^{-1} in d_0-adenine correlates with 4 transitions in d_1-adenine. According to their IR spectra (not shown here) these are the electronic origins of the NDH, NHD, N9D and CD isotopomers of 9H-adenine. The d_0-bands at 36062 and 36248 cm^{-1} however correlate with only three bands in d_1-adenine respectively. According to their IR spectra these bands arise from overlapping transitions of the NDH+N9D isotopomers (the redmost d_1-electronic transition of the 3 bands system is somewhat broader and approximately two times more intense than the other transitions), the NHD and the CD isotopomer. The NDH/NHD bands of the d_0-transitions at 36062 and 36248 cm^{-1} are blue shifted compared to the NDH/NHD band of the 36105 cm^{-1} transition and thus have a larger vibrational energy in the electronically excited state than the 36105 cm^{-1} transition. We recall that all 3 transitions share a common electronic ground state as the double resonance experiments show. The fact that several of the weaker d_1 bands have the 3 bands system in common argues against a deuteration shift being due simply to excitation of vibronic bands with large NH_2 displacements.

According to *ab initio* calculations at the CIS and CASSCF level the two lowest $\pi\pi^*$ states and the lowest $n\pi^*$ state are close to each other in adenine [40,41]. The intensities of the bands at 35497 and 36105 cm^{-1} are 1:34 after correction for the different laser intensities and detection sensitivities at the different wavenumbers. The ratio of oscillator strengths of the $n\pi^*$ state and the two $\pi\pi^*$ states are 1:70/370 at the CASSCF level [41] implying that the $n\pi^*$ state is the more likely candidate for the upper state of the 35497 cm^{-1} transition. The transitions at 36062, 36167 and 36248 cm^{-1} gain intensity by vibronic mixing with the electronic origin of the $\pi\pi^*$ band system at 36105 cm^{-1}. Mixing of $n\pi^*$ and $\pi\pi^*$ states and coupling of the $n\pi^*$ state to the electronic ground state has been postulated [42] as reason for the short lifetime of electronically excited adenine and its low fluorescence quantum yield. Other possible mechanisms are discussed in the chapter "photochemistry".

The ionization potential of adenine is an other important molecular property of this nucleobase. We measured the two-color/two-photon ion yield of adenine taken
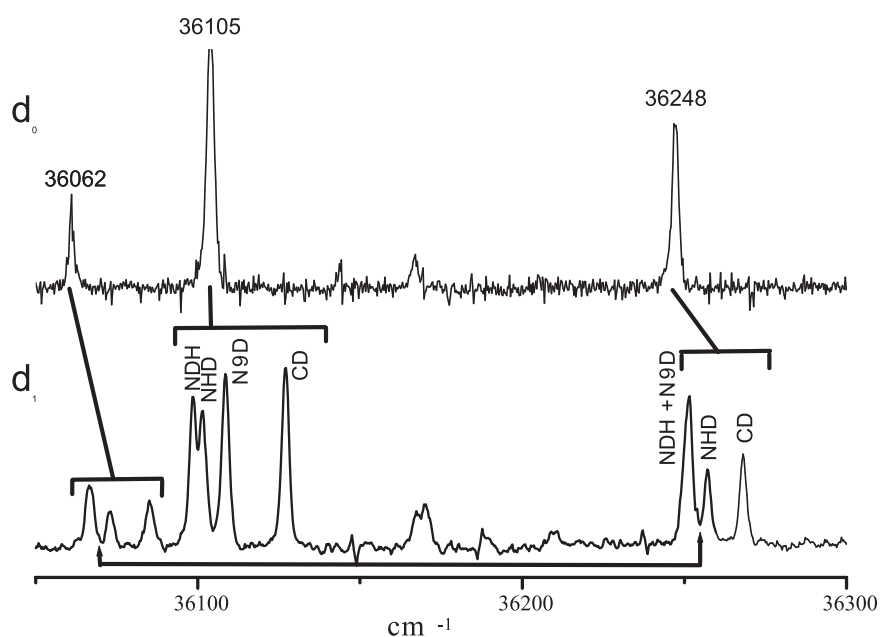
Fig. 14. R2PI spectra of undeuterated adenine and d_1-adenine. For explanation see text.

via the electronic resonance at $36\,105$ cm^{-1} as function of the frequency of the ionization laser. Zero time jitter between the two excitation lasers turned out to be necessary for efficient ionization of the short lived excited state [24] of adenine. This was achieved by pumping two dye lasers with the same Nd–YAG laser. The ionization colors were obtained from two dyes: DCM ($33\,100$–$34\,200$ cm^{-1}) and Rhodamin 6G/B ($33\,600$–$34\,400$ cm^{-1}). The ion signal was corrected for the laser energy in these ranges. After correction for field ionization we obtain $69\,400 \pm 50$ cm^{-1} (8.606 ± 0.006 eV) for the vertical ionization potential of jet-cooled 9H-adenine which is probably near to the adiabatic IP. This can be compared to 8.45 eV obtained from electron impact ionization of gas phase adenine [43]. Similarly we obtained an ionization potential of $63\,760 \pm 20$ cm^{-1} (7.905 ± 0.002 eV) for 7H-enolguanine. Hole transfer through DNA involves positive charges moving between guanines, the DNA bases with the lowest ionization potential, by tunneling at short distances and by thermally induced hopping of charges between adenine bases at long distances [44]. Precise ionization potentials of the nucleobases may contribute to better understand this process.

3.8 Comparison of properties of the nucleobases and their dimers

The picture that emerges from these data is still incomplete but it does allow us to draw several conclusions about the photochemistry of the bases and about their pairing properties.

3.8.1 Photochemistry and dynamics

All nucleobases involved in replication have very low fluorescence and phosphorescence quantum yields associated with excited-state lifetimes of the order of picoseconds [45,46] and sub-picoseconds in recent investigations of nucleotides and nucleosides in the liquid phase [47,48]. Quenching occurs by internal conversion to the ground state [48]. It has been argued that evolution has arrived at this particular choice of building blocks for its genetic machinery, because the short lifetime protects them from photochemistry [42].

In the gas phase electronically excited 9H-adenine exhibits ps lifetime [24] and shows a rather narrow spectrum while the redmost absorbing enol and keto tautomers of guanine have ns lifetimes [30] and quite extended spectra. The biologically relevant 9-methylguanine in the keto form however could not be detected [31] similar as keto guanosine possibly again due to a too short lifetime in the excited electronic state. 9-methyladenine shows an even more narrow spectrum than 9H-adenine [49] implying that the coupling to interfering excited states takes place already at lower vibronic energies and that its lifetime is short again.

7H-enolguanine and 2-aminopurine (9H/7H tautomer distribution not yet known) have nanosecond lifetimes [30,50] and absorb further to the red than the 9H tautomer of 6-aminopurine (adenine) and 9H-enolguanine.

A model to qualitatively explain these data involves multiple electronic states with initial excitation to a $\pi\pi^*$ state which interacts with at least one other excited state. The relative positions of these states determine the extent and the energy at which predissociation can take place such that a lower $\pi\pi^*$ state not only means absorption further to the red but can also lead to a different coupling with the interfering excited states. Uracil and thymine exhibit broad structureless absorption, suggesting especially strong mixing in the excited state [5].

Broo and others [42] have proposed that the interfering excited state is of $n\pi^*$ character and that it couples with the ground state to provide a pathway for radiationless quenching. More recently Sobolewski and Domcke have proposed that a $\pi\sigma^*$ excited state may be instrumental in coupling the $\pi\pi^*$ state with the ground state *via* a conical intersection [51]. The $\pi\sigma^*$ potential is repulsive with respect to the stretching of OH and NH bonds and promotes hydrogen transfer to a protic solvent [51]. Indeed we observe the electronic spectra of GC, G–G9M, CC, C–C1M and A–A also on the C+H, G9M+H, C+H, C1M+H and A+H masses respectively, although weaker. We currently perform delayed 2-color ionization experiments to check if the H transfer indeed takes place in the electronically excited state of the neutral cluster or if a proton transfer takes place in the ionic ground state. We are undertaking to study clusters with water to further elucidate these issues.

Preliminary data of a cluster of 9-ethylguanine with 1-methylcytosine shows a broad structureless absorption suggesting once again effective interactions in the excited state. This is particularly interesting because this cluster is a model for the nucleoside base pair since the substitutions are in the positions of the sugar moiety.

3.8.2 Base pairing

When studying the pairing of individual bases, a major question is whether we observe the calculated lowest energy hydrogen bonded structures. Higher levels of computation are as yet available only for certain base pair combinations and the experimental results can serve as a calibration for such *ab initio* calculations [39]. For most combinations we studied so far only lower levels of computation are feasible. The general trend is that the structures that we observe are among the lowest energy structures according to our calculations. However certain structures appear to be missing. One example is the symmetric G–G structure, which was discussed above. In this case it is conceivable that very different hydrogen bond strengths in the S_0 and S_2 state and to some extent also exciton splitting cause a large wavelength blue shift and possibly too little stability in the excited S_2 state. Other unobserved structures include certain tautomer combinations. In the case of the G–G dimers we only observed structures with a keto-guanine (G_k) and none with enol-guanine (G_e). From the monomer spectroscopy we know that both tautomeric forms are present in the beam. This suggests that enol dimers and mixed dimers should be formed as well. The fact that the binding energy of G_e–G_e is much less than that of G_k–G_k is irrelevant, since those refers to different populations in the beam. One would expect to find the respective lowest energy structure for each type of dimer, with relative abundances depending on the relative monomer abundances.

The most conspicuous missing combination is that for the Watson-Crick (WC) structure of the GC pair. The structure that we observed is identical to WC, except that the C is in the enol tautomeric form. From our results on cytosine we know that C is present in our beam both as keto- and as enol-C in similar abundances. Thus it appears that the mere move of a hydrogen in C causes the keto WC structure to go unobserved. There are a number of possible explanations.

(1) The cluster is not formed. This is unlikely because it is predicted to be the most stable structure. If the cluster is formed with enol cytosine, surely it would be expected to be formed with keto cytosine as well.

(2) It goes undetected because of a large wavelength shift. This is unlikely if we assume that keto guanine is the chromophore both in the detected GC cluster and the WC GC pair. If we are ionizing these clusters through the cytosine chromophore however, a large difference in wavelength could be possible between the cluster with the keto versus the enol C.

(3) A short lifetime of the intermediate excited state could reduce the R2PI signal. In that case the question arises why the lifetime would be so different for two so similar clusters.

(4) The ion could be unstable. Once again we would then have to ask for the difference between the enol and keto ionic cluster. We are currently undertaking various double resonance experiments to test these different scenarios.

Whichever will turn out to be the underlying chemistry, the apparent special characteristics of the GC keto WC structure is very intriguing.

References

1. I.K. Yanson, A.B. Teplitsky, L.F. Sukhodub, Biopolymers **18**, 1149 (1997)
2. S.P. Fodor, R.P. Rava, R.A. Copeland, T.G. Spiro, J. Raman Spectr. **17**, 471 (1986)
3. H. Urabe, H. Hayashi, Y. Tominaga, Y. Nishimura, K. Kubota, M. Zsuboi, J. Chem. Phys. **82**, 531 (1985)
4. S. Cocco, R. Monasson, J. Chem. Phys. **112**, 10017 (2000)
5. B.B. Brady, L.A. Peteanu, D.H. Levy, Chem. Phys. Lett. **147**, 538 (1988)
6. M.R. Viant, R.S. Fellers, R.P. Mc Laughlin, R.J. Saykally, J. Chem. Phys. **103**, 9502 (1995)
7. R.D. Brown, P.D. Godfrey, D. McNaughton, A.P. Pierlot, J. Chem. Soc., Chem. Commun. **1**, 37 (1989)
8. K. Liu, R.S. Fellers, M.R. Viant, R.P. McLaughlin, M.G. Brown, R.J. Saykally, Rev. Sci. Instrum. **67**, 410 (1996)
9. M.R. Viant, R.S. Fellers, R.P. McLaughlin, R.J. Saykally, J. Chem. Phys. **103**, 9502 (1995)
10. P. Colarusso, K. Zhang, B. Guo, P.F. Bernath, Chem. Phys. Lett. **269**, 39 (1997)
11. R.D. Brown, P.D. Godfrey, D. McNaughton, A.P. Pierlot, J. Am. Chem. Soc. **110**, 2329 (1988)
12. W. Caminati, G. Maccaferri, P.G. Favero, L.B. Favero, Chem. Phys. Lett. **251**, 189 (1996)
13. S. Keun Kim, W. Lee, D.R. Herschbach, J. Phys. Chem. **100**, 7933 (1996)

14. R.D. Brown, P.D. Godfrey, D. McNaughton, A.P. Pierlot, J. Am. Chem. Soc. **110**, 2308 (1989)
15. E. Nir, L. Grace, B. Brauer, M.S. de Vries, J. Am. Chem. Soc. **121**, 4896 (1999)
16. E. Nir, Ch. Janzen, P. Imhof, K. Kleinermanns, M. de Vries, J. Chem. Phys. **115**, 4604 (2001)
17. F. Piuzzi, M. Mons, I. Dimicoli, B. Tardivel, Q. Zhao, Chem. Phys. **270**, 205 (2001)
18. M. Mons, I. Dimicoli, F. Piuzzi, B. Tardivel, M. Elhanine, J. Phys. Chem A **106**, 5088 (2002)
19. E. Nir, K. Kleinermanns, M. de Vries, Nature **408**, 949 (2000)
20. E. Nir, Chr. Janzen, P. Imhof, K. Kleinermanns, M.S. de Vries, Phys. Chem. Chem. Phys. **4**, 740 (2002)
21. E. Nir, Chr. Janzen, P. Imhof, K. Kleinermanns, M.S. de Vries, Phys. Chem. Chem. Phys. **4**, 732 (2002)
22. E. Nir, P. Imhof, K. Kleinermanns, M.S. de Vries, J. Am. Chem. Soc. **122**, 8091 (2000)
23. N.J. Kim, G. Jeong, Y.S. Kim, J. Sung, S.K. Kim, J. Chem. Phys. **113**, 10051 (2000)
24. D.C. Lührs, J. Viallon, I. Fischer, Phys. Chem. Chem. Phys. **3**, 1827 (2001)
25. Chr. Plützer, E. Nir, M.S. de Vries, K. Kleinermanns, Phys. Chem. Chem. Phys. **3**, 5466 (2001)
26. E. Nir, M. Müller, L.I. Grace, M.S. de Vries, Chem. Phys. Lett. **355**, 59 (2002)
27. G. Meijer, M.S. de Vries, H.E. Hunzicker, H.R. Wendt, Appl. Phys. B **51**, 395 (1990)
28. Ch. Janzen, D. Spangenberg, W. Roth, K. Kleinermanns, J. Chem. Phys. **110**, 9898 (1999)
29. *Gaussian 98*, Revision A.4, M.J. Frisch, G.W. Trucks, H.B. Schlegel, P.M.W. Gill, B.G. Johnson, M.A. Robb, J.R. Cheeseman, T. Keith, G.A. Petersson, J.A. Montgomery, K. Raghavachari, M.A. Al-Laham, V.G. Zakrzewski, J.V. Ortiz, J.B. Foresman, J. Cioslowski, B.B. Stefanov, A. Nanayakkara, M. Challacombe, C.Y. Peng, P.Y. Ayala, W. Chen, M.W. Wong, J.L. Andres, E.S. Replogle, R. Gomperts, R.L. Martin, D.J. Fox, J.S. Binkley, D.J. Defrees, J. Baker, J.P. Stewart, M. Head-Gordon, C. Gonzalez, J.A. Pople, Gaussian, Inc., Pittsburgh PA, 1995
30. F. Piuzzi, M. Mons, I. Dimicoli, B. Tardivel, Q. Zhao, Chem. Phys. **270**, 205 (2001)
31. M. Mons, I. Dimicoli, F. Piuzzi, B. Tardivel, M. Elhanine, J. Phys. Chem A **106**, 5088 (2002)
32. K. Szczepaniak, M. Szczesniak, W. Szajda, W.B. Person, J. Leszczynski, Can. J. Chem. **69**, 1705 (1991)
33. K. Schoone, G. Maes, L. Adamowicz, J. Mol. Struct. **480**, 505 (1999)
34. A. Held, D.W. Pratt, J. Am. Chem. Soc. **112**, 8629 (1990)
35. E.G. Robertson, J.P. Simons, Phys. Chem. Chem. Phys. **3**, 1 (2001)
36. M. Schmitt, Ch. Jacoby, M. Gerhards, C. Unterberg, W. Roth, K. Kleinermanns, J. Chem. Phys. **113**, 2995 (2000)
37. M. Gerhards, C. Unterberg, K. Kleinermanns, Phys. Chem. Chem. Phys. **2**, 5538 (2000)
38. Y. Matsuda, T. Ebata, N. Mikami, J. Chem. Phys. **110**, 8397 (1999) and references therein
39. M. Kabelac, P. Hobza, J. Phys. Chem. B **105**, 5804 (2001)
40. B. Menucci, A. Toniolo, J. Tomasi, J. Phys. Chem. A **105**, 4749 (2001)
41. M.P. Fülscher, L. Serrano-Andres, B.O. Roos, J. Am. Chem. Soc. **119**, 6168 (1997)
42. A. Broo, J. Phys. Chem. A **102**, 526 (1998)
43. S.K. Kim, W. Lee, D.R. Herschbach, J. Phys. Chem. **100**, 7933 (1996)
44. B. Giese, J. Amaudrut, A.-K. Köhler, M. Spormann, St. Wessely, Nature **412**, 318 (2001)
45. D.N. Nikogosyan, D. Angelov, S. Benoit, L. Lindqvist, Chem. Phys. Lett. **252**, 322 (1996)
46. A. Reuther, H. Iglev, R. Laenen, A. Laubereau, Chem. Phys. Lett. **325**, 360 (2000)
47. J. Peon, A.H. Zewail, Chem. Phys. Lett. **348**, 255 (2001)
48. J.-M.L. Pecourt, J. Peon, B. Kohler, J. Am. Chem. Soc. **123**, 10370 (2001)
49. Chr. Plützer, K. Kleinermanns, Phys. Chem. Chem. Phys. (to be published, 2002)
50. C. Santosh, P.C. Mishra, Spectrochim. Acta A **47**, 1685 (1991)
51. A.L. Sobolewski, W. Domcke, C. Dedonder-Lardeux, C. Jouvet, Phys. Chem. Chem. Phys. **4**, 1093 (2002)
52. M. Gerhards, C. Unterberg, Appl. Phys. A **72**, 273 (2001)
53. J.B. Foresman, Æleen Frisch, *Exploring Chemistry with Electronic Structure Methods*, 2nd edn. (Gaussian Inc., 1996)